Eur. Phys. J. B (2019) 92: 121
https://doi.org/10.1140/epjb/e2019-90415-5

THE EUROPEAN PHYSICAL JOURNAL B

Regular Article

Structural, spectral and optical properties of rocksalt Al,Mn-doped CdO: experimental and DFT studies

Asli A. Kaya[1,a] and Kadir Erturk[2]

[1] Department of Physics, Faculty of Art and Science, Bilecik Seyh Edebali University, Bilecik, Turkey
[2] Department of Physics, Faculty of Art and Science, Namik Kemal University, Tekirdag, Turkey

Received 25 June 2018 / Received in final form 4 April 2019
Published online 10 June 2019

Abstract. Nano-crystalline $Cd_{0.95-x}Mn_{0.05}Al_xO$ (x = 0, 0.02, 0.04, 0.06, 0.08, 0.10) semiconductors were synthesized by sol-gel technique. These samples are characterized via X-ray diffraction (XRD), scanning electron microscope (SEM) and Fourier-transform infrared spectroscopy (FTIR) methods. XRD analyses show that the samples have pure rocksalt structure, which is typical for cadmium oxide (CdO). SEM micrographs show that the Al,Mn-doped CdO nanoparticles are cubic with rocksalt structures. The presence of bands at 499, 615 and 660 cm^{-1} observed in the FTIR spectrum correspond to the stretching of CdO. In addition, the optical properties of nanoparticles were performed as experimentally and theoretically. The optical band gaps of nanoparticles were measured between 1.87 and 2.34 eV, while calculated as 1.19 eV for Mn-doped CdO nanoparticle and 2.13 eV for Mn,Al-doped CdO nanoparticle at lanl2dz and pm6 basis sets. The optical studies showed that the Mn-doped reduces band gap, while Al-doped increases.

1 Introduction

Cadmium oxide (CdO) is an n-type semiconductor in which the band gap of approximately is 2.5 eV [1]. It is thought that this structure of CdO provides many superior properties. The CdO films have been successfully used for many applications, including phototransistors [2], gas sensor [3], solar cells [4], liquid crystal displays, IR detectors and antireflection coatings [5]. For this reason, it is an important that this semiconductor is obtained in a pure form. These thin films can be synthesized by different methods such as sol-gel [6], spray pyrolysis [7].

The sol-gel method has many advantages because it is simple to apply, easy to control, low costly and safely. It is also easy to doping different elements. The CdO thin films which are doped various elements such as Sn [8], In [9] and Al [10] have already been studied. There are many experimental and theoretical studies on CdO nanoparticles in the literature, but the effect of Mn and Al doped on optical and surface properties has not been found. In this study, nano-crystalline $Cd_{0.95-x}Mn_{0.05}Al_xO$ (x = 0, 0.02, 0.04, 0.06, 0.08, 0.10) semiconductors were synthesized by sol-gel technique. Incorporation of Mn and Al into the CdO structure was confirmed by energy-dispersive X-ray, scanning electron microscope (SEM) and Fourier-transform infrared spectroscopy (FTIR) analysis. The samples were also annealed at 500 and 600 °C for improvement of sample morphology properties. In addition, the optical band gaps of nanoparticles were determined from absorption spectra, and theoretical optical properties were performed using time-dependent density functional theory (TDDFT) method and lanl2dz and pm6 basis sets.

On the other hand, both CdO and diluted magnetic semiconductors play the key role for spintronic technology. It is desirable to produce spintronic devices based on controls of electron turns rather than electronic charges with diluted magnetic semiconductors. Spintronic devices provide many advantages such as higher speed, lower power consumption and functionality than traditional devices. Al and Mn-doped CdO is a powder material in the class of the dilute magnetic semiconductor commonly researched today. In this research, Al and Mn-doped CdO powders have been produced as diluted magnetic semiconductors suitable for use in spintronic devices and investigated the experimental and theoretical properties of these DMSs.

2 Experimental procedure

In the present work, nano-crystalline $Cd_{0.95-x}Mn_{0.05}Al_xO$ (x = 0, 0.02, 0.04, 0.06, 0.08, 0.10) powder samples were synthesized via sol-gel method. Cadmium acetate dihydrate [$Cd(CH_3COO)_2{\cdot}2H_2O$], manganese nitrate [$Mn(NO_3)_2{\cdot}6H_2O$], aluminum nitrate [$Al(NO_3)_3{\cdot}6H_2O$] and citric acid ($C_6H_8O_7$) were used for powder productions. The appropriate molar ratios of the chemicals were separately dissolved in 100 ml of distilled water. The aqueous solutions were then mixed by vigorous stirring

[a] e-mail: asli.kaya@bilecik.edu.tr

for about 60 min. The pH of the aqueous solutions was continuously monitored and maintained at 7.0 by adding an appropriate amount of liquid ammonia. The xerogel of the solution was attained by constant stirring and evaporation at 200 °C on a hot plate. The samples annealed at 500 and 600 °C were used in experimental measurements. Structural and optical characterizations of nano-crystalline $Cd_{0.95-x}Mn_{0.05}Al_xO$ ($x = 0$, 0.02, 0.04, 0.06, 0.08, 0.10) powder samples were performed by energy-dispersive X-ray [X-ray diffraction (XRD)], SEM and UV–Vis spectra analysis.

3 Theoretical procedure

The x, y, z coordinates of the optimized structure of the rocksalt $Cd_{32}O_{32}$ cluster were taken from reference [11]. These optimized structural parameters have been used in all calculations. The $Cd_{31}MnO_{32}$ cluster was obtained by placing Mn atom instead of Cd atom, and the instead of two Cd atoms, Mn and Al atoms were combined to form the $Cd_{30}MnAlO_{32}$ cluster. The lowest singlet vertical excitation energies of each clusters and the UV–Vis absorption spectra are then subsequently calculated using TDDFT/B3LYP method with lanl2dz basis set and semi-empirical method with pm6 basis set on the ground state geometries. The band gaps with Mn and Al doped clusters are defined as the difference between the calculated energies for the lowest unoccupied molecular orbital (LUMO) and highest occupied molecular orbital (HOMO). All calculations were carried out using Gaussian 09 software packed [12]. All molecular structures and HOMO–LUMO molecular orbitals were visualized with GausView software [13].

4 Results and discussions

All samples were firstly characterized by XRD diffraction analysis. The XRD patterns of all samples were measured before annealing procedure, but results indicate the amorphous structure for all powders. After then, the amorphous structure of these powders is altered by annealing effect and the changes in the structure were measured by X-ray analysis. Only the CdO phase is present, which indicates either a total insertion of the dopant ions into the CdO crystal lattice or a secondary phase that is so small that it is unobservable in XRD measurements. Figure 1 shows the XRD patterns of as-synthesized Al-doped CdMnO samples, annealed at 500 and 600 °C. The (111), (200), (220) and (311) reflections are clearly seen and are very close to the reference patterns for CdO [JCPDS: 05-0640]. All the patterns are found to be in pure rocksalt structure and are not affected by Al doping. Furthermore, the 2θ values of the most intense peak are not altered with the increase in the Al concentration.

The SEM micrographs of synthesized nanoparticles of $Cd_{0.95-x}Mn_{0.05}Al_xO$ ($x = 0$, 0.02, 0.04, 0.06, 0.08, 0.10) are shown in Figure 2. The SEM structures obtained are similar to those reported by earlier workers [10,14] for Al-doped CdO. These micrographs reveal the high crystalline

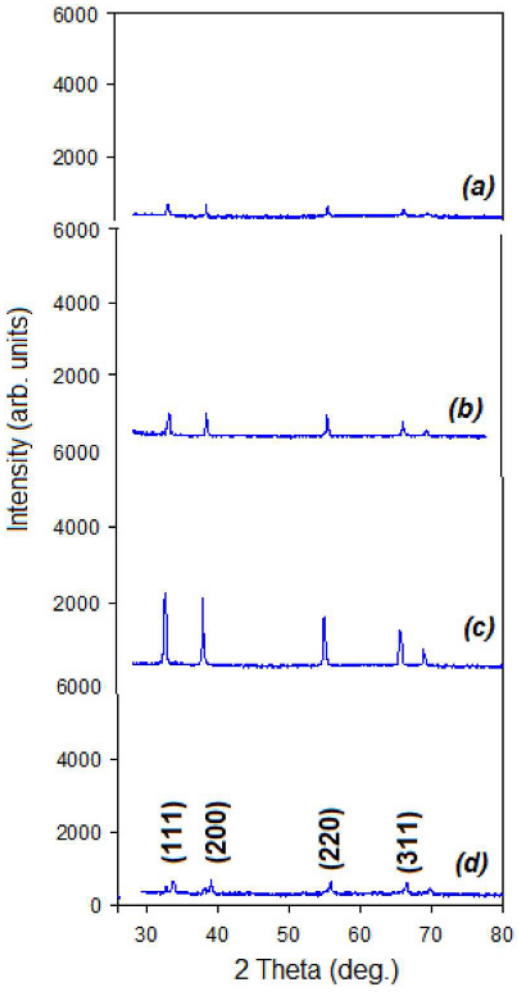

Fig. 1. XRD spectra of (a) $Cd_{0.91}Mn_{0.05}Al_{0.04}O$ (500 °C), (b) $Cd_{0.91}Mn_{0.05}Al_{0.04}O$ (600 °C), (c) $Cd_{0.89}Mn_{0.05}Al_{0.06}O$ (500 °C) and (d) $Cd_{0.89}Mn_{0.05}Al_{0.06}O$ (600 °C).

in these samples, whereas some particles do not seem to be monodisperse. The samples annealed at 600 °C showed more homogeneous structure. The particles are observed to be somewhat agglomerated in higher concentration samples.

The other characterization method of CdO nanoparticles is FTIR. FTIR analysis is an effective tools used to identify the functional groups present in the studied material. The FTIR spectra of Mn-doped CdO nanoparticle were taken by using a Perkin Elmer Spectrum Two FTIR spectrophotometer with 450–4000 cm^{-1}. Figure 3 shows the FTIR spectrum of Mn-doped CdO nanoparticle. The band at 3000–3600 cm^{-1} as a broad band corresponds to adsorbed water molecule [15]. The CH stretching vibration was observed at 3013 and 2964 cm^{-1}. The bands at 1545 and 1388 cm^{-1} are associated with stretching mode of CO and bending of CH group, respectively. The band corresponding to C–O–H bending plane is observed at 933 cm^{-1}. These vibration modes belong to carboxylic acid. The characteristic bands in the range of 400–700 cm^{-1} correspond to CdO vibration modes [16]. In the FTIR spectra, the characteristic vibration modes of CdO nanoparticle were measured at 499, 615 and

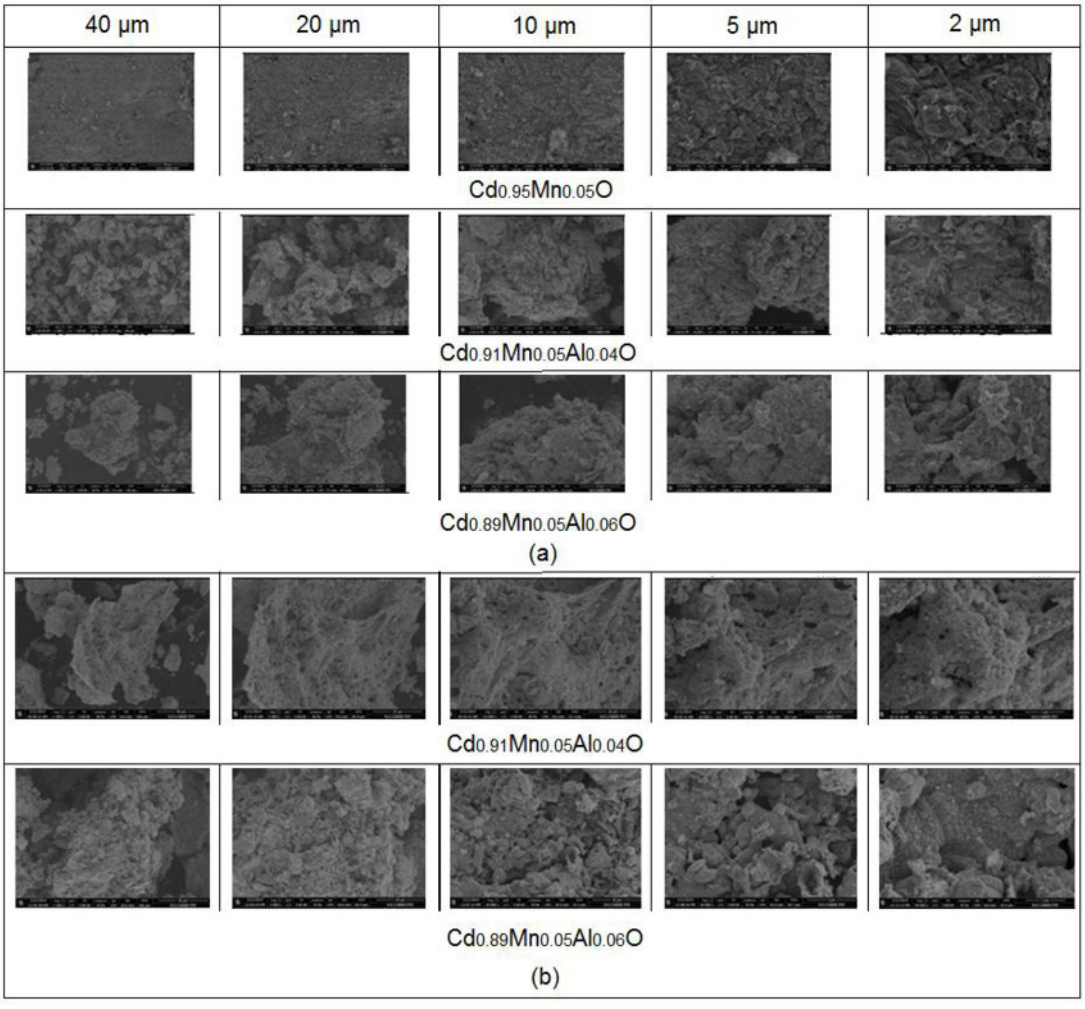

Fig. 2. SEM micrographs of $Cd_{0.95}Mn_{0.05}O$, $Cd_{0.91}Mn_{0.05}Al_{0.04}O$ and $Cd_{0.89}Mn_{0.05}Al_{0.06}O$ samples (a) annealed at 500 °C and (b) annealed at 600 °C.

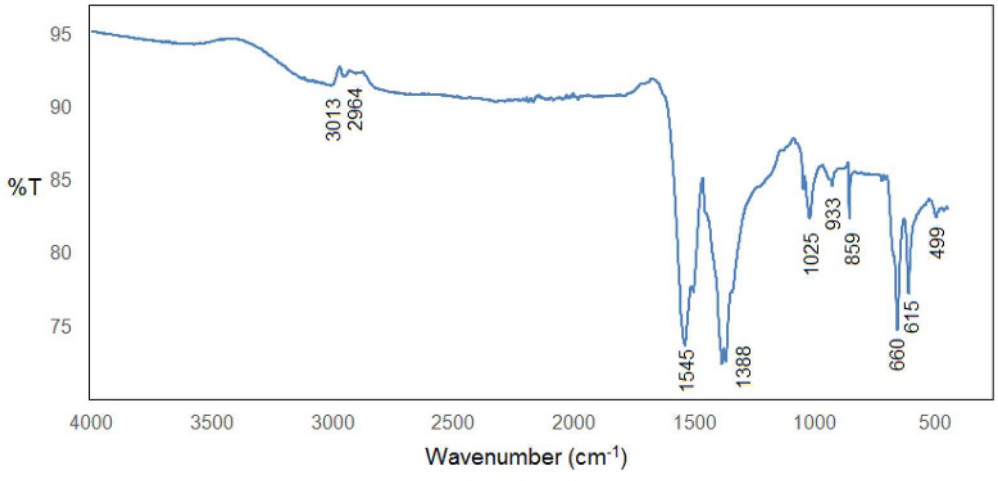

Fig. 3. FTIR spectra of Mn-doped CdO nanoparticle.

660 cm^{-1}. These results indicate the formation of CdO nanoparticles.

The absorption coefficient for the Al,Mn-doped CdO powder samples, $Cd_{0.95-x}Mn_{0.05}Al_xO$ ($x = 0$, 0.02, 0.04,

0.06, 0.08, 0.10) can be used to estimate the type of transition and the optical band gap energy according to Tauc's relationship [17]

$$\alpha h\nu = (A/h\nu)(h\nu - E_g)^r$$

where A is a proportionality constant, E_g is the energy band gap and r is a constant which depends on probability of transition; $r = 1/2$ and $3/2$ for direct transitions, $r = 2$ and 3 indirect transitions. The dependence of $(\alpha h\nu)^{1/r}$ on photon energy $h\nu$ was plotted for different values of r. The best fit was obtained for $r = {}^1/_2$ and this result pointed out that the transitions are direct allowed transitions. Therefore, the direct band gaps of the Al,Mn-doped CdO samples can be found by the extrapolated linear regression of the curve resulting from a plot of $(\alpha h\nu)^2$ vs. photon energy $(h\nu)$, and displayed in Figure 4. The band gaps are measured at 1.87 eV for $Cd_{0.95}Mn_{0.05}O$ sample, while the Al-doped $Cd_{0.95-x}Mn_{0.05}Al_xO$ ($x = 0$, 0.02, 0.04, 0.06, 0.08, 0.10) samples were observed at 2.25, 2.32, 2.07, 2.34 and 2.17 eV, respectively. On the other hand, the experimentally band gap of CdO is approximately 2.5 eV in the literature [1]. These results indicate that the optical band gap of CdO is lowered by Mn-doped and increased by Al-doped. The strong exchange interactions between the s and p electrons of Al ions and the d electrons of the host matrix cause some changes in the optical properties. The d–s and d–p exchange interactions could give rise to a negative and positive correction to the conduction and the valance-band edges, caused band gap to expanded. At the same time, it was found that aluminum added at different concentrations had no regular effect on the band gap, that is, the band gap did not increase regularly with the increase in Al-concentration.

In the theoretical calculations, the optimized structure and geometry parameters of the $Cd_{32}O_{32}$ cluster taken from the reference [11] were used, and the average bond distance between Cd and O atom was calculated at 2.348 Å in this geometry. All of clusters contain 64 atoms are shown in Figure 5a. In theoretical calculations for band gaps of Al,Mn-doped CdO clusters, $Cd_{32}O_{32}$, $Cd_{31}MnO_{32}$ and $Cd_{30}MnAlO_{32}$, the TDDFT/B3LYP/lanl2dz and semi-empirical/pm6 levels were chosen for optical calculations, since the TDDFT/B3LYP method is the more accurate method for calculating the optical properties of these type metal oxides in the literature [11,18] and the semi-empirical/pm6 method is considered to be the closest to DFT method. The valance-electron configurations for the elements of rocksalt CdO are Cd $4d^{10}5s^2$ and O $2s^22p^4$. The band gap is calculated as theoretically from energy difference between HOMO and LUMO [19]. It is useful to note that the calculations fall close to experimental values, while we are not concerned with replicating absolute band gap energies. The band gap energies of $Cd_{32}O_{32}$, $Cd_{31}MnO_{32}$ and $Cd_{30}MnAlO_{32}$ clusters were calculated with lanl2dz basis set as 1.71, 1.19 and 2.13 eV, respectively, and performed with pm6 basis set as 2.25, 2.40 and 3.52 eV, respectively. The band gap of CdO nano-crystal was observed as approximately 2.5 eV [1], while the band gap energies of the Mn-doped CdO and Al,Mn-doped CdO were measured as 1.87 and 2.07–2.34 eV, respectively. The measured band gaps were generally observed higher than the calculated values. But, as a result of the calculations, the optical band gap of CdO is lowered by Mn-doped, and increased by Al-doped. These results confirm the experimental study. In addition, the TDDFT/B3LYP/lanl2dz method calculations give better results than semi-empirical/pm6 calculations in doped CdO band gap calculations, while the semi-empirical/pm6 method gave closer result for band gap of undoped CdO as seen in Table 1.

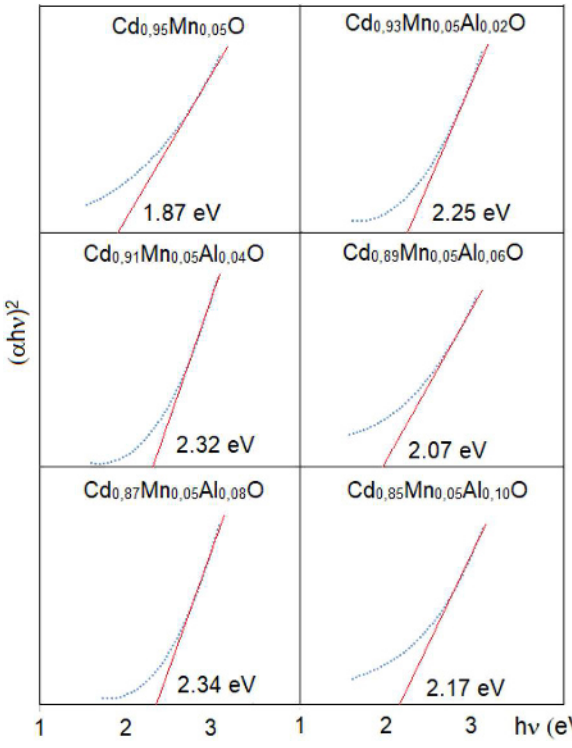

Fig. 4. The relation between $(\alpha h\nu)^2$ and photon energy $(h\nu)$ of the $Cd_{0.95-x}Mn_{0.05}Al_xO$ ($x = 0$, 0.02, 0.04, 0.06, 0.08, 0.10).

As seen in Figure 5b, the HOMO and LUMO of $Cd_{32}O_{32}$ cluster are situated mostly O atoms. In the Mn-doped CdO cluster, the electron density of HOMO mainly localized over Mn, Cd and O atoms, while the LUMO is situated Cd and O atoms. In addition to the $Cd_{30}MnAlO_{32}$ cluster, the Al atom also provides an additive on HOMO and LUMO. To support the accuracy of calculations and to further understand of the effect of Mn and Al doped, the total density of states (DOS) were calculated at pm6 level as seen in Figure 6. The DOS calculations revealed the symmetry of the HOMO and LUMO orbitals of $Cd_{32}O_{32}$ cluster are T2 and A1, respectively. In addition, calculation DOS plots in Figure 6 show that neither valence nor conduction levels of the tube are significantly changed after Mn and Al doped, so these results also support experimental and other theoretical calculations.

5 Conclusions

The Mn and Al,Mn-doped CdO samples were prepared from by sol-gel method and characterized by using XRD,

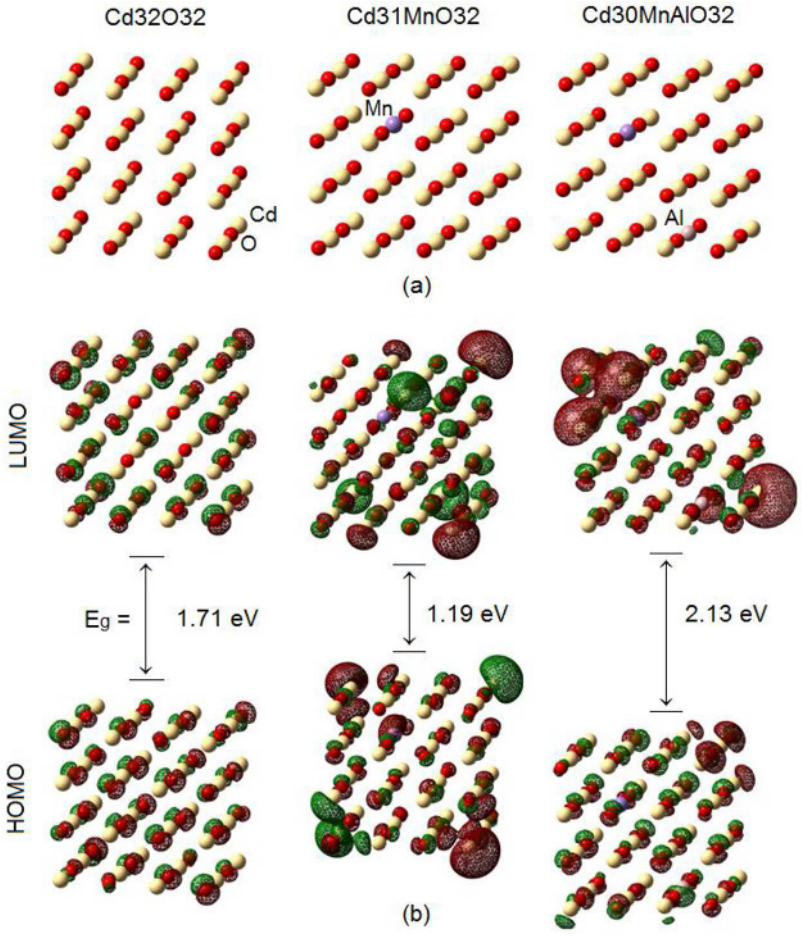

Fig. 5. (a) Molecular structure, (b) HOMO, LUMO and band gap of $Cd_{32}O_{32}$, $Cd_{31}MnO_{32}$ and $Cd_{30}MnAlO_{32}$ clusters.

Table 1. Experimental and theoretical band gaps of CdO, Mn-doped CdO and Mn,Al-doped CdO nanoparticles.

Nanoparticles	Experimental (eV)	lanl2dz (eV)	pm6 (eV)
CdO	2.50 [1]	1.71	2.46
$Cd_{0.95}Mn_{0.05}O$	1.87	1.19	2.40
$Cd_{0.93}Mn_{0.05}Al_{0.02}O$	2.25	2.13	3.52
$Cd_{0.91}Mn_{0.05}Al_{0.04}O$	2.32		
$Cd_{0.89}Mn_{0.05}Al_{0.06}O$	2.07		
$Cd_{0.87}Mn_{0.05}Al_{0.08}O$	2.34		
$Cd_{0.85}Mn_{0.05}Al_{0.10}O$	2.17		

SEM and FTIR techniques for the study of structural and morphological properties, respectively. The optical properties were performed as experimentally and theoretically. According to the results,

(i) Mn-doped CdO and Mn,Al-doped CdO samples were synthesized as amorphous, and these samples turned to crystalline from amorphous structure as a result of annealing.
(ii) XRD patterns show the formation of pure rocksalt structure for all samples.
(iii) The samples annealed at 600 °C showed more homogeneous structure.
(iv) The presence of bands at 499, 615 and 660 cm^{-1} observed in the FTIR spectrum correspond to the stretching of CdO.
(v) The band gaps are measured at 1.87 eV for $Cd_{0.95}Mn_{0.05}O$ sample, while the Al-doped $Cd_{0.95-x}Mn_{0.05}Al_xO$ ($x = 0$, 0.02, 0.04, 0.06, 0.08, 0.10) samples were observed between 2.07 and 2.34 eV. The optical band gap of CdO is lowered by Mn-doped, and increased by Al-doped.
(vi) The theoretical results from obtained TDDFT and DOS calculations confirm the experimental study.

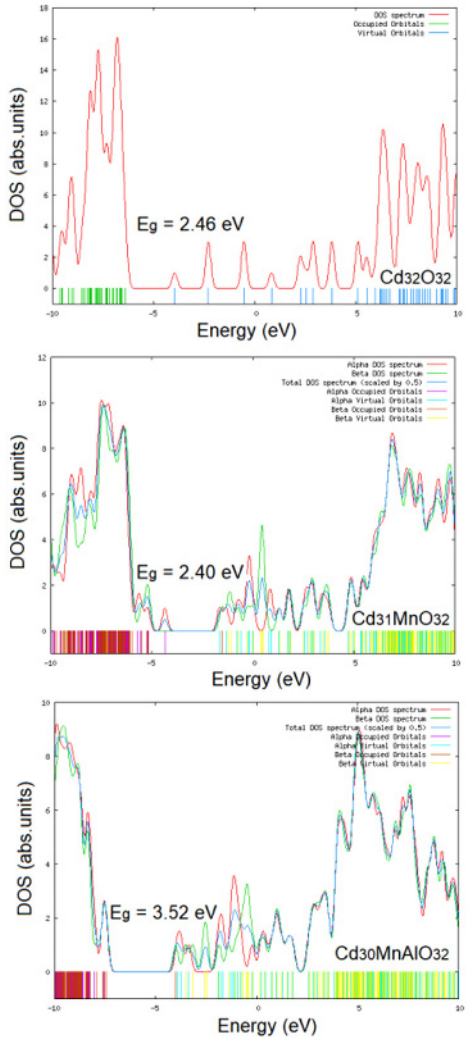

Fig. 6. DOS spectra of $Cd_{32}O_{32}$, $Cd_{31}MnO_{32}$ and $Cd_{30}MnAlO_{32}$ clusters.

This work is a part of a research Projects OUAP(F)-2013/14 and KUAP (F)-2013/25. We thank Uludag University for the financial support given to the projects. The authors would like to acknowledge Dr. Yunus Kaya for their kind help in experimental and theoretical procedure.

Author contribution statement

Asli Kaya conceived the subject, prepared the samples, carried out the FTIR, optical analysis and computational studies. Kadir Erturk performed XRD, SEM analysis and helped in the Results and Discussion section. Both authors contributed to the writing of the manuscript, have read and approved the final manuscript.

References

1. D.M. Carballeda-Galicia, R. Castanedo-Perez, O. Jimenez-Sandoval, S. Jimenez-Sandoval, G. Torres-Delgado, C.I. Zuniga-Romero, Thin Solid Films **371**, 105 (2000)
2. L.M. Su, N. Grote, F. Schmitt, Electron. Lett. **20**, 716 (1984)
3. R.R. Salunkhe, C.D. Lokhande, Sens. Actuators B **129**, 345 (2008)
4. T.L. Chu, S.C. Shirley, J. Electron. Mater. **19**, 1002 (1990)
5. I.M. Ocampo, A.M. Ferandez, P.J. Sabastian, Semicond. Sci. Technol. **8**, 750 (1993)
6. J. Santos-Cruz, G. Torres-Delgado, R. Castanedo-Perez, S. Jimenez-Sandoval, J. Marquez-Marin, O. Zelaya-Angel, Sol. Energy **80**, 142 (2006)
7. C.H. Bhosale, A.V. Kambale, A.V. Kokate, K.Y. Rajpure, Mater. Sci. Eng. B **122**, 67 (2005)
8. L.R. de León-Gutiérrez, J.J. Cayente-Romero, J.M. Peza-Tapia, E. Barrera-Calva, J.C. Martínez-Flores, M. Ortega-López, Mater. Lett. **60**, 3866 (2006)
9. R.K. Gupta, K. Ghosh, R. Patel, S.R. Mishra, P.K. Kahol, Mater. Lett. **62**, 3373 (2008)
10. R. Maity, K.K. Chattopadhyay, Sol. Energy Mater. Sol. Cells **90**, 597 (2006)
11. M.C.C. Wobbe, M.A. Zwijnerburg, Phys. Chem. Chem. Phys. **17**, 28892 (2015)
12. M.J. Frisch, G.W. Trucks, H.B. Schlegel, G.E. Scuseria, M.A. Robb et al., *Gaussian 09, Revision D.01* (Gaussian Inc., Wallingford, 2009)
13. R. Dennington, T. Keith, J. Millam, K. Eppinnett, W.L. Hovell, R. Gilliland, *GaussView, Version 3.07* (Semichem Inc., Shawnee Mission, KS, 2003)
14. A. Abdolahzadeh Ziabari, F.E. Ghodsi, G. Kiriakidis, Surf. Coat. Technol. **213**, 15 (2012)
15. J. Singh, P. Kumar, K.S. Hui, K.N. Hui, K. Raman, R.S. Tiwari, O.N. Srivastava, CrystEngComm **14**, 5898 (2012)
16. B. Malecka, A. Lacz, Thermochim. Acta **479**, 12 (2008)
17. M.M. El-Nahass, A.A. Atta, M.M. Abd El-Raheem, A.M. Hassanien, J. Alloys Compd. **585**, 1 (2014)
18. A.A. Peyghan, M. Noei, Physica B **432**, 105 (2014)
19. D.F.V. Lewis, C. Loannides, D.V. Parke, Xenobiotica **24**, 401 (1994)